DESIGN AND ANALYSIS OF SOI MEMS VOLTAGE STEP UP CONVERTERS

R. Gleeson, M. Kraft and N.M White
Electronics and Computer Science, University of Southampton, Southampton, UK

Abstract: This paper presents a comprehensive analysis of voltage step-up converters for energy harvesting and other low-power applications. The step-up operation is based on isolating the charge of a mechanically variable capacitor and varying the gap between the electrodes by an appropriate method of providing an actuation force. Two devices are presented; a bi-stable device and a resonant device, specifically designed for static and resonant energy harvesting respectively. The bi-stable device introduces a separate electrostatic actuator element to manipulate the variable capacitor electrodes, whereas, in the case of the resonant device, ambient vibrations provide the necessary actuation force. The devices were then fabricated using a dicing-free Silicon-on-Insulator (SOI) process.

Keywords: MEMS Voltage Conversion, Energy Harvesting, SOI

INTRODUCTION

Self-sufficient devices, which eliminate the need for an external voltage source, are becoming a popular area of interest. Much research has and is being done in the field of energy harvesting devices which generate power from external ambient sources e.g. solar, wind, vibration etc. However, these harvesters often produce relatively low voltages (<1V) compared to the requirements of the intended application [1]. To address the issues in voltage discrepancy, various voltage multiplication techniques have been introduced.

Within the past two decades, a significant amount of research has been conducted in the field of Micro-Electro Mechanical systems (MEMS). Accelerometers and gyroscopes have been popular areas of research during this time. In such devices, ambient acceleration causes a displacement of a proof mass, which may be represented as a capacitor electrode, thus causing a change in capacitance. The same methodology of mechanically varying levels of capacitance has been further developed as a method of creating a new form of MEMS voltage converter. The operation on which these converters are based on is relatively straightforward; if a mechanically variable capacitor is kept at a constant charge, Q, and its electrodes are displaced by an external force, the voltage, V, across the capacitor, C will increase according to Q=C*V.

There have been several previous theoretical investigations [2-5] into these devices with few real devices being fabricated and little information regarding power efficiency, which is a critical factor for energy harvesting. In this paper, two single-stage multiplier devices are presented; a bi-stable and a resonant device. The bi-stable device features an electrostatic actuation element while the resonant device relies on ambient vibrations to provide the actuation force. For energy harvesting, it is of the utmost importance that the end devices are designed to exhibit high levels of power efficiency and relatively low levels of parasitic capacitance to compete with existing multiplier circuits. This paper presents the initial analysis and operation of these devices; however, the future focus of this work is to optimize electrical efficiency.

THEORY

The operation of a MEMS voltage converter is based on a mechanically variable capacitor. A circuit level representation for this device is shown in fig.1. Initially, the capacitor electrodes are brought to a distance g_{min} resulting in maximum capacitance C_{max} as it charges up to the input voltage V_{in}. An external actuation force then pulls apart the capacitor electrodes until an electrode distance g_{max} with minimum capacitance C_{min} is reached. This action increases the voltage across the capacitor and it simultaneously discharges to the load. The cycle then repeats. The multiplication factor of the device is given by $M = C_{max}/C_{min}$.

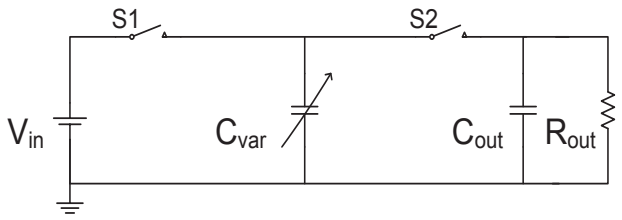

Fig. 1: Converter circuit overview. C_{var} is the mechanically varying capacitor driven by non overlapping switches S1 and S2.

Bi-stable Device

In this design, a parallel plate actuator is used to drive apart the electrodes of a comb drive capacitor. The 2nd order equation dictating this motion is given by:

$$mg'' + bg' + k(g_0 - g) = F_{EL} \quad (1)$$

Where k represents the spring constant, b is the damping co-efficient, g is the displacement, g_0 is the "at rest" gap, m is mass and F_{EL} is the electrostatic force which is given as a difference between the force generated by the capacitor (F_{EL1}) and the actuator (F_{EL2}). The formulae for the forces generated by capacitor and actuator, respectively, are given as follows:

$$F_{EL1} = \frac{NT\varepsilon_0 V^2}{g} \quad (2)$$

$$F_{EL2} = \frac{\varepsilon_0 A V^2}{2g^2} \quad (3)$$

Here, N is the number of comb fingers, T is the thickness of the electrodes, A is electrode area and V is the input voltage. The input voltage is assumed to be 24V, which is a typical output for static solar power generators.

Resonant Device

By replacing the electrostatic actuator element in the previous design with a proof mass, the system can make use of ambient vibrations to provide actuation. The resonant frequency of the mechanical system can be designed to match the frequency of vibration using the formula:

$$\omega_0 = \sqrt{\frac{k}{m}} \quad (4)$$

Where $\omega_0 = 2\pi f_0$ and f_0 is the resonant frequency. The devices presented in this work are designed to work with low frequency vibrations (<300Hz) as many vibration energy harvesters operate on low frequencies [3]. The actuation force in this case is given by F=ma.

SIMULATION

Simulated output voltage results for the bi-stable device are shown in Fig. 2. The red line represents the ideal output of the system for M=5. This is found using virtual diodes, in place of S1 and S2 of Fig. 1, and an infinite load resistance. Once the diodes are replaced for a more realistic 1N4148 model, there is an issue with leakage current and the output drops considerably. If a 100MΩ load resistance is added to model a typical oscilloscope probe, the output will spike. This is due to the load resistance being too low and so current leaks through the probe. To avoid this spiking effect, a significantly higher load resistance (≈1GΩ) is needed.

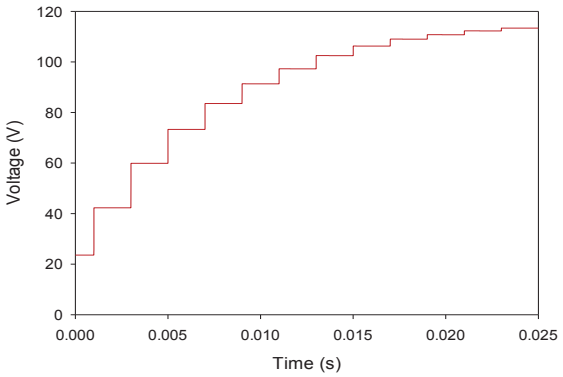

Fig. 2: Output voltage of bi-stable device. (red) ideal output with infinite load resistance and virtual diodes for M=5, (green) output with 1N4148 diodes in the circuit and 100MΩ load.

3D models of the converter devices were created in MEMS+ and transferred to Conventorware for analysis. These models are shown in Fig. 3 and 4.

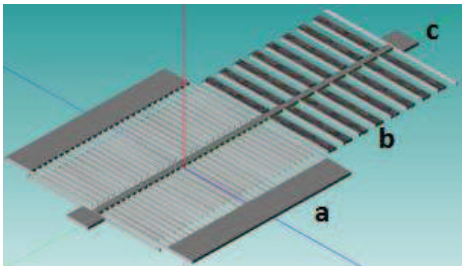

Fig. 3: MEMS+ model of bi-stable device (a) parallel plate actuator, (b) comb drive capacitor, (c) anchor and spring.

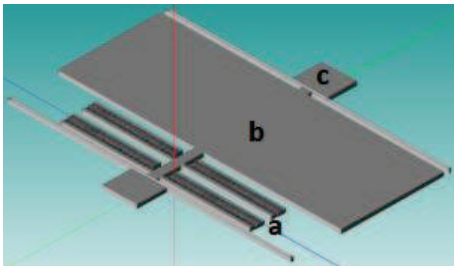

Fig. 4: MEMS+ model of resonant device (a) comb drive capacitor, (b) proof mass (c) anchor and spring.

Parasitic capacitances will adversly affect the multiplication factor. For a comb capacitor, fringing fields make up the bulk of these parasitics. As the minimum electrode overlap distance (g_{min}) increases, the effect of these fringing fields becomes reduced. However, the electrostatic force also increases and so the actuator size must increase to compensate. Therefore, there is a trade off between choosing a value of g_{min} to achieve a reasonable multiplication factor without consuming too much area. For this work, g_{min} = 7µm which results in M≈3.

Table 1: Effect of minimum electrode overlap gap on voltage multiplication factor. Ideally the capacitor has been designed for M=5.

g_{MIN}	C_{MAX}	C_{MIN}	M
2µm	.1237pF	.06868pF	1.8
7µm	.475	.15pF	3.16
10µm	.65pF	.188pF	3.45
20µm	1.69pF	.4pF	4.255

FABRICATION

The devices presented have been designed to be fabricated using Silicon on Insulator (SOI). Etch holes, backside and frontside trenches were used to allow for the complete release of the device from the wafer by etching [6]. This work incorporates the addition of an oxide mask to eliminate the need for a carrier wafer during the patterning of the delicate front side features.

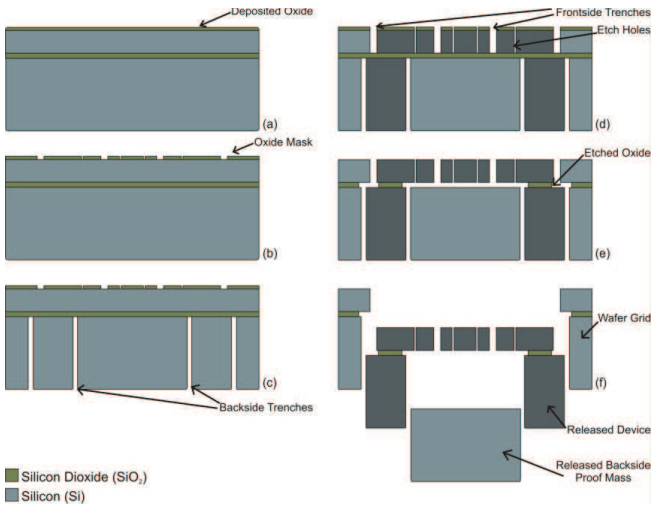

Fig. 5: Removal process: (a) 1µm layer of SiO_2 is deposited using PECVD, (b) SiO_2 is patterened and etched to create a hard mask, (c) backside trenches are patterend and defined using DRIE, (d) frontside features are defined using DRIE, (e) buried oxide and hard mask layer etched in HF VPE, (d) device seperation.

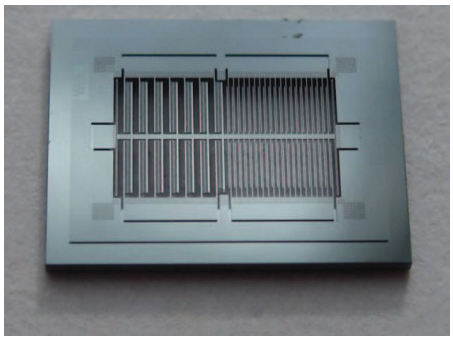

Fig. 6: Front side camera image of released bi-stable device.

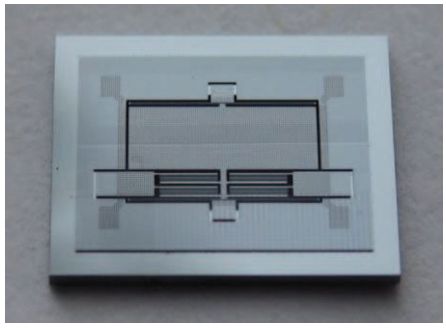

Fig. 7: Front side camera image of released resonant device.

MEASUREMENT

The circuit in Fig. 1 was constructed using 1N4148 diodes in place of the switches to replicated the Multisim models. A 100MΩ was used in place of the load resistor. The switching of the actuator was preformed using a solid state relay mosfet switch. The output voltage for this arrangement is shown in fig. 9.

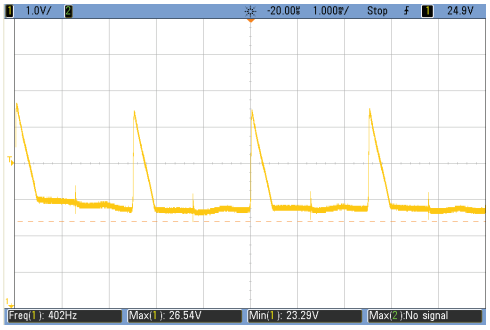

Fig. 8: Measured voltage output using 1N4148 diodes in control circuit and 100MΩ oscilloscope probe lead.

This response is a close match to the simulated output shown in Fig. 2. The peak value is slightly lower due to leakage and parasitics in the circuit. If the load resistance was increased, less leakage will occur. To demonstrate this, a high impedance path

was created using an AD8610 op-amp unity gain buffer. The resulting output is shown in Fig. 9.

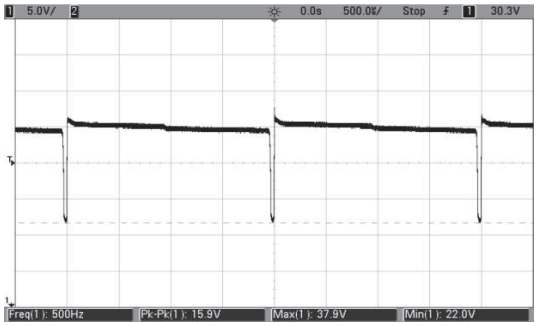

Fig. 9: Measured voltage output but with the addition of a unity gain op-amp buffer at the output.

The opamp was operated using a separate 40V supply voltage and so the output will only reach a maximum peak of 40V. The addition of a power supply for this op-amp is clearly not ideal. In order to prove that the converters will provide full multiplication under the correct load conditions while maintaining a single 24V input supply voltage, a voltage divider network is used to lower the output voltage at the input to the unity gain buffer. The circuit configuration for this is shown in Fig. 10 and the simulated output is shown in Fig. 11. For this analysis, a voltage divider was used to scale down the voltage by a factor of 6.

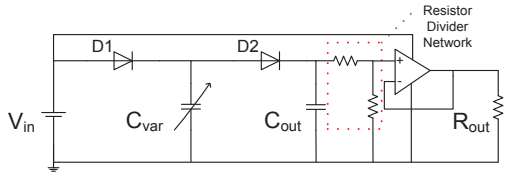

Fig. 10: Measured voltage output but with the addition of a unity gain op-amp buffer at the output.

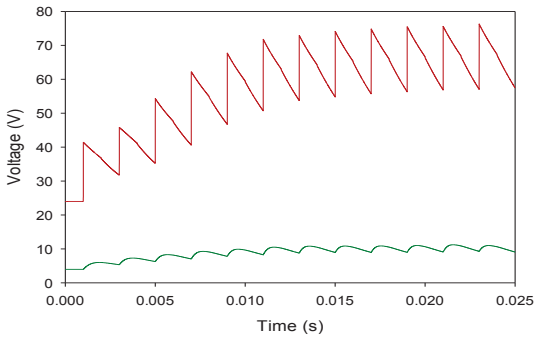

Fig. 11: Output voltage of bi-stable device with 1N4148 diodes, (red) infinite load resistance, (green) arrangement of Fig.10 with resistor divider, unity gain buffer and 100MΩ load.

CONCLUSION

MEMS voltage converters for energy harvesting applications have been presented and analyzed. The main issues with these devices are parasitic capacitances and leakage currents. The parasitic capacitances of both the capacitor (fringing fields) and the diode switches (junction capacitance) cause attenuation in the maximum achievable multiplication factor. The resistance of both the diodes and load cause current from the capacitor to leak away between charging. For load resistances below 1GΩ, the current will not flow through the load capacitor but leak straight through the resistor. It is possible to counteract this leakage by increasing the size, and thus capacitance, of the capacitor so it will store more current and can be operated at a higher frequency to increase the charging speed. However, this dramatically affects the area of the device as the actuator must also increase to compensate for the increased electrostatic force generated by the capacitor. It has been shown that by using a unity gain buffer, the output can achieve maximum multiplication. This maximum level is limited by the parasitic capacitance present in the diodes.

REFERENCES

[1] El Hami M., Glynne-Jones P., White N. M., Beeby S., James E., Brown A. D. and Ross J. N. 2001 Design and fabrication of a new vibration-based electromechanical power generator *Sensors and Actuators A* **92** 335-42

[2] Haas C. and Kraft M. 2003 Modeling and analysis of a MEMS based approach to a voltage step-up conversion, *J.Micromech. Mircoeng.***14** 114-22

[3] Ghandour S., Despesse G. and Basrour S. 2009 Theoretical analysis of a new MEMS approach to build a high efficiency fully integrated DC-DC converter, *Proc. MME*

[4] O' Mahoney C. and Hill M. 2006 Modeling and performance evaluation of a MEMS DC/DC converter *J. Mircomech. Microeng*. **16** 149–55

[5] Li L., Begbie M. and Uttamchandani D. 2007 Single-input, dual-output MEMS DC/DC converter *Electronics Letters* **43**

[6] Sari I., Zeimpekis I. and Kraft M. 2010 A full wafer dicing free dry release process for MEMS devices *Proc. Eurosensors XXIV*